Surface & Coatings Technology 388 (2020) 125590

Contents lists available at ScienceDirect

Surface & Coatings Technology

journal homepage: www.elsevier.com/locate/surfcoat

Self-lubricating Cu-MWCNT coatings deposited from an ecofriendly glutamate-based electrolyte

Leandro N. Bengoa[a], Pablo R. Seré[a], Paola Pary[a,*], M. Susana Conconi[b], José M. Folgueiras[c], Eneas N. Morel[c], Jorge Torga[c], Walter A. Egli[a]

[a] Centro de Investigación y Desarrollo en Tecnología de Pinturas-CIDEPINT (CICPBA-CONICET-UNLP), Av. 52 121 y 122 s/n, B1900AYB La Plata, Argentina
[b] Centro de Tecnología de Recursos Minerales y Cerámica-CETMIC (CICPBA-CONICET), Cno. Centenario y 506, B1897ZCA, M.B. Gonnet, Argentina
[c] Laboratorio de Optoelectrónica y Metrología Aplicada, UTN - FACULTAD REGIONAL DELTA, Av San Martin 1171 (2804), Campana, Buenos Aires, Argentina

ARTICLE INFO

Keywords:
Copper
Carbon nanotubes
Composite
Friction
Tribology

ABSTRACT

Self-lubricating coatings have been studied for a long time due to their convenience compared to systems which need periodic lubrication. For this reason, Cu-CNT composite coatings with high wear resistance and low coefficient of friction were obtained by electrodeposition from an ecofriendly alkaline glutamate-based electrolyte. Deposition experiments were performed at various experimental conditions in the presence of low-frequency ultrasound agitation to ensure particle dispersion and enhance their incorporation in the Cu matrix. Moreover, the effect of 2-Butyne-1,4-diol (an additive use in glutamate-based formulations) on coatings mechanical and tribological properties was assessed. Both pure Cu and Cu-CNT were obtained under all the experimental conditions considered and later characterized by SEM and XRD. Finally, pin-on disk tests were performed to estimate the coefficient of friction and determine the wear resistance. The results showed that incorporation of CNT to the copper matrix led to an improvement of the tribological performance of pure Cu, regardless of deposition parameters. Furthermore, it was found that 2-Butyne-1,4-diol had a strong influence on deposit microhardness and tribological performance, as a result of the changes in microstructure induced by this additive which promoted the development of a (111) texture. Likewise, the incorporation of particles to the Cu matrix promoted changes in surface morphology as well as in the preferred crystalline orientation, promoting crystal growth along the [311] direction. The results indicate that this simple and cheap methodology is suitable for fabrication of self-lubricating coatings.

1. Introduction

The development of self-lubricating coatings has been an issue of interest to the scientific and engineering community for a long time. The use of these kind of deposits eliminates the need of periodic lubrication [1] making these materials very convenient for long-term operation. Consequently, several alternatives to produce such coatings have been proposed and investigated, among which powder metallurgy [2,3], electroless [4,5] and electrolytic codeposition [6–9] are the most widespread ones. The latter consists in the incorporation of inert particles, which are present in the plating solution, to a metallic matrix during electrodeposition [9–11]. The result of this process is a composite coating whose properties can be tailored by choosing the right particles, bath composition and deposition parameters. This technique has been used for the synthesis of self-lubricating coatings since its discovery. In fact, the first article on composite plating dealt with the development of a copper-graphite deposit to be used in car engines [12]. Since then, many authors have studied the properties of deposits containing lubricating particles like graphite [1,6–8], PTFE [13,14] and MoS_2 [15,16].

Among the several materials that have been used for preparation of metal-based composites, carbon nanotubes (CNTs) stand out for their excellent mechanical properties (high tensile strength and elastic modulus) [17] as well as low coefficient of friction (**COF**) [18]. The latter have been successfully incorporated into both electroless and electrodeposited Ni [5,19–21] and Ni-P alloy [4,22], achieving a reduction in the **COF** and an increase in the microhardness of the Ni coatings. Moreover, a considerable decrease in the wear rate of both Ni-P [4] and Ni [5] coatings was observed, ascribed to the presence of loose CNTs between the surfaces in contact, released during initial stages of the wear test, which prevent their intimate contact. On the other hand, Cu-CNT composites have been the focus of several

* Corresponding author.
E-mail address: p.pary@cidepint.ing.unlp.edu.ar (P. Pary).

https://doi.org/10.1016/j.surfcoat.2020.125590
Received 10 January 2020; Received in revised form 3 March 2020; Accepted 5 March 2020
Available online 06 March 2020
0257-8972/

investigations for a while [4,23–31]. Pure copper coatings have been mainly used for protective and decorative purposes due to their good corrosion resistance and appearance, as well as in electrical or electronic applications due to copper's high electrical and thermal conductivities. However, this is a soft and heavy material [31], and thus it is not suitable for novel applications in which lightweight and high strength functional materials (e.g. with high thermal stability and high electrical conductivity) are required [30]. Therefore, it is desirable to increase Cu microhardness and wear resistance, without compromising its beneficial physical properties. Reinforcement of copper with CNTs seems to be a promising approach since, besides the extraordinary mechanical properties previously mentioned of these particles, they have high thermal and electrical conductivities [24,30] and could act as weight reducers [31]. For these reasons, many researchers have devoted their efforts to preparation of Cu-CNT composites, using either by powder metallurgy [4,23] and electrocodeposition [24–29].The resulting materials presented reasonable thermal and electrical conductivities and enhanced microhardness and tribological performance. Nevertheless, wear resistance and **COF** measurements have only been carried out on samples prepared by the former technique, and no information regarding the tribological properties of electrodeposited Cu-CNT coatings is available.

A recent review by Sundaram et al. [31] clearly remarks the influence of the synthesis route on the physical and mechanical properties of Cu-CNT composites. These differences stem from the dissimilar microstructures, particle dispersion on the metal matrix and CNT contents that can be obtained using different methodologies. For example, powder metallurgy cannot be used to produce composites with > 20 vol% CNT contents, since severe agglomeration takes place leading to a poor general performance of the material. In contrast, uniformly distributed Cu-CNT coatings can be easily achieved by electrocodeposition by adjusting the process parameters, if particles are properly dispersed in the plating solution. Several approaches have been suggested to avoid CNT agglomeration in the electrolyte [21], of which ultrasound (US) assisted electrodeposition is the most promising [32–36] as it promotes particle dispersion and incorporation into the metallic matrix at the same time. In addition to this, electrodeposition is a versatile (little geometries restrictions) and cost-effective (low vacuum or high temperatures are not required) technology and has been largely used to modify the surface properties of structural materials. Considering the advantages of this methodology over powder metallurgy, it is surprising that deposition of Cu-CNT coatings for tribological applications has not been extensively investigated.

The aim of this study is to obtain wear resistant and low **COF** Cu-CNT composites by electrodeposition from a recently developed alkaline glutamate-based electrolyte, intended to replace traditional cyanide-copper plating baths [37]. This green alternative for copper plating has already proved to be appropriate for deposition of Cu deposits of up to 10 μm, and the preparation Cu-CNT functional coatings from this eco-friendly formulation could largely boost its use and thus contribute towards a more sustainable industry. Deposition experiments were performed at various experimental conditions in the presence of low-frequency US agitation to ensure particle dispersion and enhance their incorporation in the Cu matrix. The composite coatings were later characterized, paying special attention to their mechanical and tribological performance. Pure Cu deposits were also obtained and used as benchmark material to properly evaluate the impact of CNT on coatings properties.

2. Experimental section

The electrolyte used throughout this study was a 0.2 M $CuSO_4{\cdot}5H_2O$ and 0.6 M $C_5H_8NO_4Na$ solution, prepared with reagent grade chemicals provided by Cicarelli. The pH of the electrolyte was adjusted to 8 by addition of KOH, based on previous investigations [37].

Pure copper and Cu-CNT coatings were deposited on SAE 1010 steel flat discs (50 mm in diameter and 1 mm thick) with an 11.5 mm hole in the center. These were mounted on a PTFE-wrapped steel rod and placed in the electrolyte parallel to the bottom of the cell. The anode consisted in a pure Cu sheet that covered the wall of the plating cell. Before deposition was carried out, steel disks were electrochemically cleaned in a 10% w/v NaOH at 60 °C with an anodic current density of 1 A/dm^2 for 1 min and later pickled in 10% v/v H_2SO_4 (Cicarelli, 98%) solution for 1 min at room temperature. For deposition of composite coatings, 1 g/L of HD Plas^{tm} multi-wall CNT (MWCNT) provided by Cheaptubes, with an outer diameter of 13–18 nm and lengths between 3 and 30 μm (Fig. 1), were added to the electrolyte. Some Cu and Cu-CNT deposits were obtained in the presence of 10 g/L of 2-Butyne-1,4-diol ($C_4H_6O_2$) to assess its influence on particle incorporation and the tribological properties of the resulting coatings. This additive improves adherence and appearance of Cu coatings deposited from glutamate-based plating baths, and hence is commonly used in this kind of formulations.

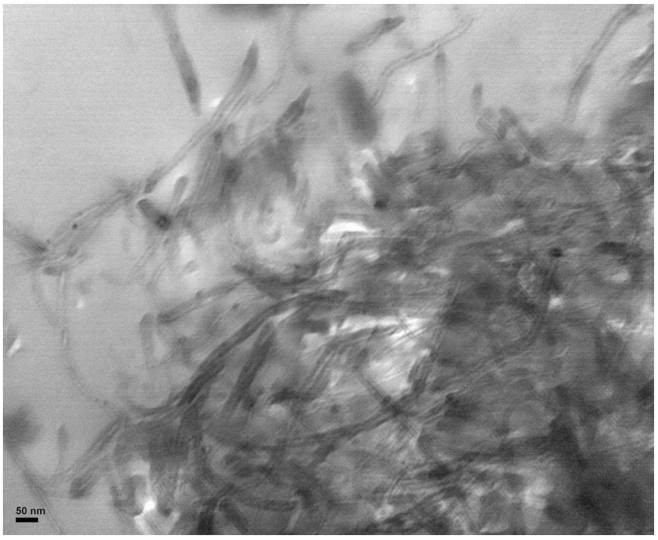

Fig. 1. TEM image of CNT used in this study.

Experiments were performed in a cylindrical cell containing 600 mL of the plating solution immersed in a Testlab TB04 ultrasonic bath (frequency: 40 kHz, nominal power: 160 W). To avoid variations on the US field applied on the reaction surface [38], the cell was always placed in the center of the US bath while the water level was controlled and kept unchanged during this study. Using this experimental set-up, the power delivered to the electrolytic cell is equal to 28 mW/cm^3, determined by the calorimetric method [35,38]. It is worth noting that ultrasonic irradiation was used both to provide electrolyte agitation and keep particles suspended and dispersed during the entire test. Therefore, no other means of agitation were used in this work. The solutions containing CNT were thoroughly stirred for at least 30 min before electrodeposition to ensure wetting and dispersion of the CNT.

Initially, the influence of temperature on the tribological performance of the deposits was evaluated. Deposits 10 μm thick were obtained at 3 A/dm^2 and temperatures in the 35–55 °C range, on steel substrates with an average roughness of R_a = 1.48 μm. These parameters are similar to those used in the industrial copper plating process of steel parts. Based on the tribological results of these samples, subsequent deposition experiments were performed at 45 °C. To evaluate the influence of the current density, tests were carried out at 1.5 and 4.5 A/dm^2. Deposits were also obtained on substrates with roughness values of 0.10 μm of R_a in order to measure the width of the wear tracks more accurately and, therefore, get a better estimation of the wear degree. Finally, higher thickness coatings (20 and 30 μm) were obtained to assess the influence of these on tribological behavior and to be able to perform microhardness and X-ray diffraction (XRD)

measurements without detecting the substrate characteristic peaks.

The morphology and chemical composition of the deposits were characterized by SEM using a Quanta200 FEI microscope (Tungsten filament source) equipped with an EDS detector. XRD measurements were performed with a Philips 3020 goniometer and a PW 3710 controller with CuKα radiation (λ = 1.54 Å) and a nickel filter. The detector was swept between 10° and 100° with a 0.04° step and 2 s per step. The patterns recorded were used to determine the preferred crystal orientation of the deposits through calculation of the relative texture coefficient (RTC) using Eq. (1), as described elsewhere [36,37,39]. For this analysis only the (200), (111), (311) and (220) planes were considered. Therefore, planes with RTC values above 25% (100/4%) are considered to be preferred crystal orientations.

$$RTC_{(hkl)} = \frac{I_{hkl}/I^0_{hkl}}{\sum_1^4 I_{hkl}/I^0_{hkl}} \times 100 \quad (1)$$

where $I(hkl)$ is the intensity of the reflection corresponding to the planes (hkl) of the tested sample and $I^0(hkl)$ is the intensity of the reflection corresponding to the planes (hkl) of a Cu powder sample with random orientation.

Moreover, the crystallite average size was estimated with FullProf Suite software, which determines this parameter describing both instrumental and sample intrinsic profile by a convolution of Lorentzian and Gaussian components using a TCH pseudo-Voigt profile function. The integral breadth method to obtain volume averages of sizes was used. In this work, the reported crystallite sizes were calculated without considering anisotropy, so they can only be used to make comparison between samples but should not be taken as accurate.

Vickers microhardness of Cu-CNT coatings was measured on the surface of the deposits using a HVS-1000B Digital Display Micro Hardness Tester, applying a 25 g load for 10 s. The values reported are the average of at least 3 measurements.

Tribological tests were carried out in a custom-made "ball on disk" tribometer applying a normal load of 2.5 N for 2 min, while the samples were rotated at 120 rpm. The counter body consisted in an AISI 52100 steel ball of 6.35 mm in diameter and 840 HV of hardness. The **COF** was calculated according to ASTM G115 from the values recorded once the friction force reached a steady value. The WD was calculated according to ASTM G99, Annex XI. Only the volume loss of the disk was determined, assuming that the due to the high hardness of the counter body it did not experience wear. This was verified by observing the ball in the microscope after each tribology test. Finally, the profiles of the wear tracks were measured with an optical profilometer depicted in Fig. 2, based on the low coherence interferometry technique [40]. The illumination source is a white light laser (NKT-SuperK Extreme EXR4) with an output power of 100 mw and a bandwidth of 200 nm (considering the limitation imposed by the detector). The output beam is launched into an optical circulator coupler. At the end of the output arm of the circulator, the light beam is collimated in an optical head and focused on a housing system [41] which contains the reference surface and the sample. The beams reflected in the reference and in the sample are detected by a spectrometer (Ocean Optics HR4000) located on the third output of the circulator, in the usual spectral domain optical coherence tomography (SD-OCT) scheme. The housing (Fig. 2-b) consists of an upper transparent window (the reference surface is the lower interface of the window), and a base were the sample is assembled. This base is fixed to a platform that allows a scanning movement in the plane normal to the optical axis of the incident beam (x-y) (Fig. 2-b). For each point of the scan, the position in this plane was measured with two encoders located in the platform (x,y). From the measurement of the interference signal, the value of the optical path difference (ΔZ_S) between the reference and the sample surface is obtained. In this way, a set of values (x, y, z) was obtained for each point selected in the scan. The platform used in this work allows scans up to 2.5 cm × 2.5 cm, with steps of 1 μm.

3. Results and discussion

Fig. 3-a shows the typical evolution of the **COF** value over time observed for Cu and Cu-CNT coatings deposited at 3 A/dm^2 in the absence of BD. For both kinds of deposits, this parameter quickly reached a stable value which remained approximately constant throughout the entire test. A similar response was obtained for Cu films deposited from a traditional acid sulfate bath, attributed to a mild wear mechanism due to low contact pressures as a result of the development of ploughing [42]. The results also show that incorporation of CNT to the Cu matrix led to a 14% decrease in the **COF**, confirming the lubricating effect of these particles. The latter can be ascribed both to the intrinsic low **COF** [18] of CNT and the presence of loose nanotubes between mating surfaces, which, due to their shape, can easily roll and slide diminishing friction forces [5]. This decrease in **COF** upon incorporation of CNT was observed for all the experimental conditions considered in this study. In this regard, it was found that the electrolyte temperature had a strong influence on **COF** value of both Cu and composite coatings (Fig. 3-b). This could be related to the development of different microstructures or textures when the deposition temperature is changed, which will affect the microhardness of the coating and thus the tribological behavior. Further investigations on this matter have not been conducted because it fell out of the scope of the present work but will be carried out in the future. However, since a minimum in **COF** was obtained at 45 °C, subsequent experiments were carried out at this temperature.

Addition of BD to the solution not only led to a rise in the steady-state **COF** value of Cu (~0.18), but also modified the tribological behavior itself. The latter is evidenced by the significant difference in the shape of the **COF** vs time curves (red curve in Fig. 4). Deposits obtained in the presence of BD showed an initial **COF** of 0.12 which steadily increased during the first half of the test until it reached a value of 0.18. The incorporation of CNT counteracted to some extent the effect of BD, leading to an almost constant lower **COF** during the entire run (~0.15). This suggests that the wear mechanism of Cu-CNT composite is likely governed by the presence of nanotubes between the sliding surfaces

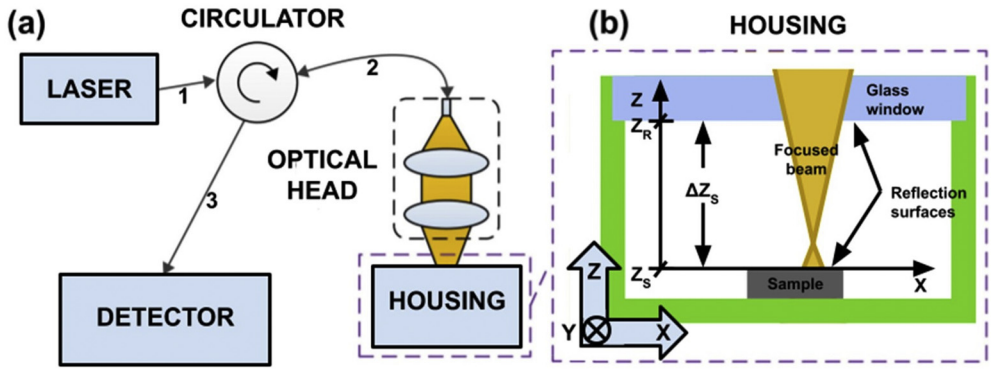

Fig. 2. (a) The laser beam after passing through the circulator (optical fibers 1 and 2) is focused into the housing. Reflections on the sample surface and on the reference window are collected by the optical head and sent back to the detector (Ocean Optics HR4000 spectrometer) by the circulator (optical fibers 2 and 3). (b) The housing consists of a glass window and a base where the sample is assembled. Two reflections, one from the lower interface of the window and the other from the upper sample surface, generate an interference signal that allows to measure the distance ΔZ_S.

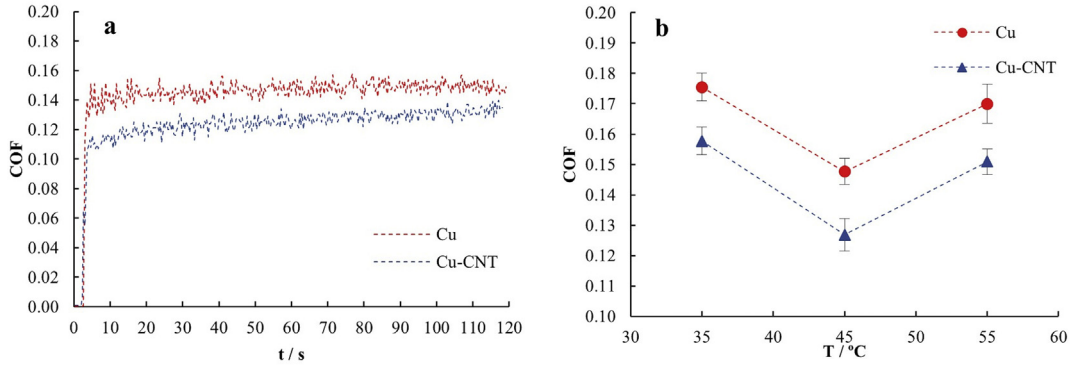

Fig. 3. (a) Evolution of COF over time of Cu and Cu-CNT deposits obtained at 3 A/dm^2 and 45 °C on steel substrates with Ra = 1.48 μm. (b) Effect of electrolyte temperature on COF value.

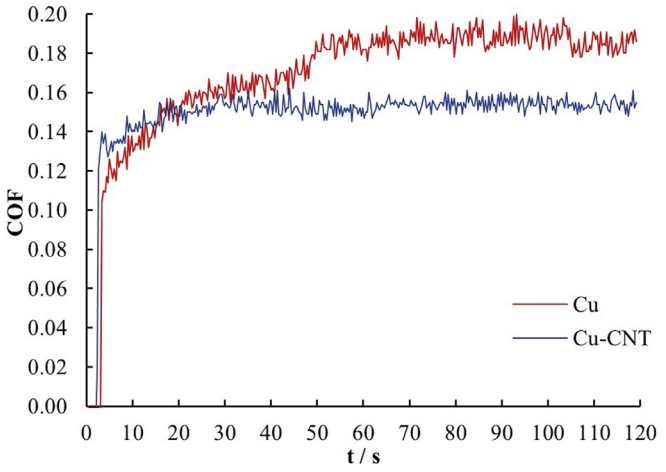

Fig. 4. Time evolution of **COF** of Cu and Cu-CNT deposits obtained at 3 A/dm^2 and 45 °C in an electrolyte containing 10 g/L of BD on steel substrates with R_a = 1.48 μm.

rather than the properties of the metal matrix. Nevertheless, BD still has some influence on the tribological performance of this coatings since it led to an increase in the average **COF** of Cu-CNT from 0.13 (Fig. 3) to 0.15.

Fig. 5 summarizes the effect of BD, CNT incorporation and current density on the performance of Cu deposited from a glutamate-based electrolyte. The results show that regardless of experimental conditions,

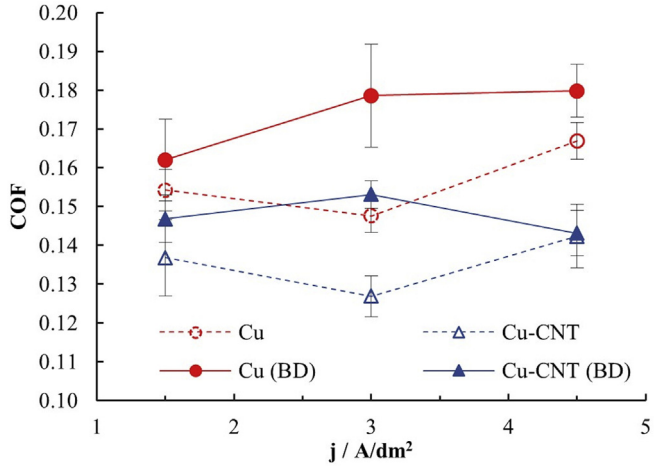

Fig. 5. COF of Cu and Cu-CNT obtained at different current densities at 45 °C in the presence and the absence of BD.

CNTs improved the lubricating properties of Cu coatings. In contrast, the effect of current density on **COF** depended on whether BD was present in the solution or not. For samples obtained in a BD-free solution, the minimum **COF** value was reached at 3 A/dm^2 for Cu and Cu-CNT. On the contrary, an increase in this parameter was observed for deposits obtained in the presence of BD when current density was raised from 1.5 to 3 A/dm^2. Further increase in current density up to 4.5 A/dm^2 did not induce significant variations in the **COF** of Cu (BD) samples but led to a slight decrease for Cu-CNT (BD) samples. This may be attributed to a higher amount of CNT in the composite obtained at 4.5 A/dm^2 which would translate into further improvement in the tribological properties. In fact, it was at these experimental conditions (4.5 A/dm^2 and with BD) that the most significant reduction in **COF** upon incorporation of CNT was observed, supporting the idea of a higher incorporation rate mentioned before. It is worth mentioning that the **COF** values registered are similar to those reported for Cu-CNT composites synthesized by powder metallurgy [4]. Some additional features about the trends depicted in Fig. 5 can be made. First, the decrease in **COF** reached by the incorporation of CNT in the absence of BD is approximately the same regardless of current density. These results may indicate that the CNT content remained constant throughout the current density range under consideration. In contrast, the beneficial effect of CNT on the lubricating properties of Cu coatings became more significant at higher current densities after addition of BD to the electrolyte, which could mean that the number of particles in the composite increases whit this parameter. The different behaviors observed with and without BD, might be explained considering Fransaer et al. mechanism for particle codeposition [43]. According to these authors, water molecules adsorbed at the electrode surface hinder particle-electrode contact, affecting the incorporation rate. For that reason, the highest particle content is achieved when the net charge of the electrode is zero (i.e. potential of zero charge, E_{PZC}), condition at which the hydration layer is loosely attached to the metal surface [44] and hence water molecules can be easily removed by an incoming particle. However, it is well known that organic compounds adsorption usually reaches a maximum in the vicinity of E_{PZC} [45,46], competing with particles for a place at the surface of the growing deposit. The latter could change the dependence of particle content with current density (or electrode potential), which may account for the trends observed in this study.

The results discussed up to this point correspond to deposits obtained on substrates with Ra = 1.48 μm, which allowed for a proper characterization of the influence of several variables on the **COF** of both Cu and Cu-CNT. However, even though the wear tracks on these samples were well-defined, precise determination of WD and wear mechanism were not possible due to surface irregularities. For this reason, deposition was performed on steel cathodes with an average roughness of 0.10 μm at 3 A/dm^2 and 45 °C, conditions at which the best **COF** value was obtained. Moreover, the morphology and microstructure of

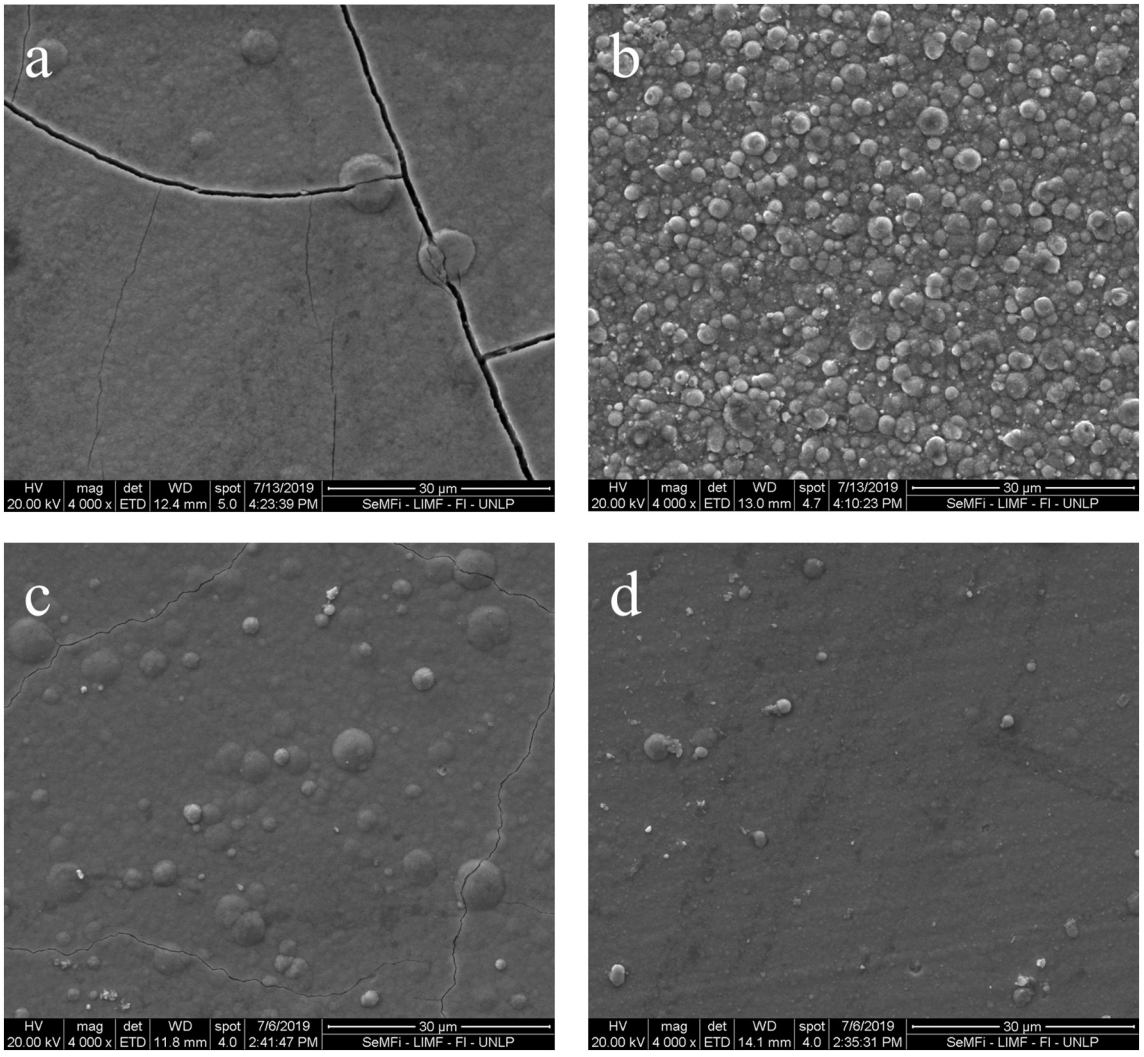

Fig. 6. SEM images (4000×) of Cu and Cu-CNT coatings deposited at 3 A/dm^2 and 45 °C on smooth substrates in the absence of BD: (a) Cu and (b) Cu-CNT; and in the presence of BD: (c) Cu and (d) Cu-CNT.

these coatings was analyzed in order to better understand the differences in the tribological behavior.

The morphology of a copper coating deposited from an electrolyte without BD is shown in Fig. 6-a. This deposit presented a smooth cracked surface with some large nodules, in line with previous results [37]. Incorporation of CNT to Cu matrix, led to development of a highly globular morphology consisting of small rounded peaks (Fig. 6-b) similar to that observed by Arai et al. [24,25]. These authors provided a detailed explanation of the growth mechanism of Cu-CNT composites, according to which at high current densities (> 2 A/dm^2) the tips of previously incorporated CNT can act as nucleation sites onto which copper grows with a spherical geometry. Newly arrived CNTs may be embedded at these copper regions instead of the main deposit, propagating this bumpy morphology all over the coating surface. It should be remarked that this deposition process can take place thanks to CNTs high electrical conductivity along their axis. Fig. 6-c and -d shows that the morphology of Cu and Cu-CNT deposits obtained in the presence of BD is like the one of copper coatings deposited without addition of this compound. However, only small cracks were detected on Cu deposits, which indicates that this additive prevents their formation. Moreover, comparison of Fig. 6-b and -d suggests that BD might act as a levelling agent that hinders Cu deposition on the tip of CNT avoiding the development of a bumpy morphology. It is worth mentioning that due to their size, it was not possible to see these particles in the Cu matrix even at high magnifications. However, the increase in carbon content, estimated by EDS, of samples with and without CNT from nearly 0 at.% to 13 at.%, together with changes in morphology and microstructure (see following paragraphs) confirm CNT incorporation. Furthermore, large particle agglomerates were not detected either on the surface or the cross-section (not shown), proving the effective dispersal of particles in the electrolyte achieved by US agitation.

To determine the preferred crystal orientation, XRD patterns were recorded (Fig. 7) and the $RTC_{(hkl)}$ for each sample were calculated. The results (Fig. 8) showed that in the absence of BD, Cu deposition took place following mainly the [311] and [220] directions, since both planes presented $RTC_{(hkl)}$ values above 25%. The latter indicates that US irradiation affects the electrocrystallization process inducing a change in the preferred crystal orientation of Cu deposits changing the texture from (111) [37] to a (311) and (220). This effect has been already observed during Zn [35] and Ni [38] composites electrodeposition. It can be seen in Fig. 8 that the incorporation of CNT to the copper matrix led to an increase in the $RTC_{(311)}$ value and a decrease in $RTC_{(220)}$, further promoting the development of a (311) texture. Although the influence of embedded particles in the microstructure of electrodeposited coatings has been previously reported [34,47–49], the underlying mechanism is still unclear. Several explanations have been proposed so far, all of which could be considered plausible. This relies on the fact that the particle chemistry and physical properties will

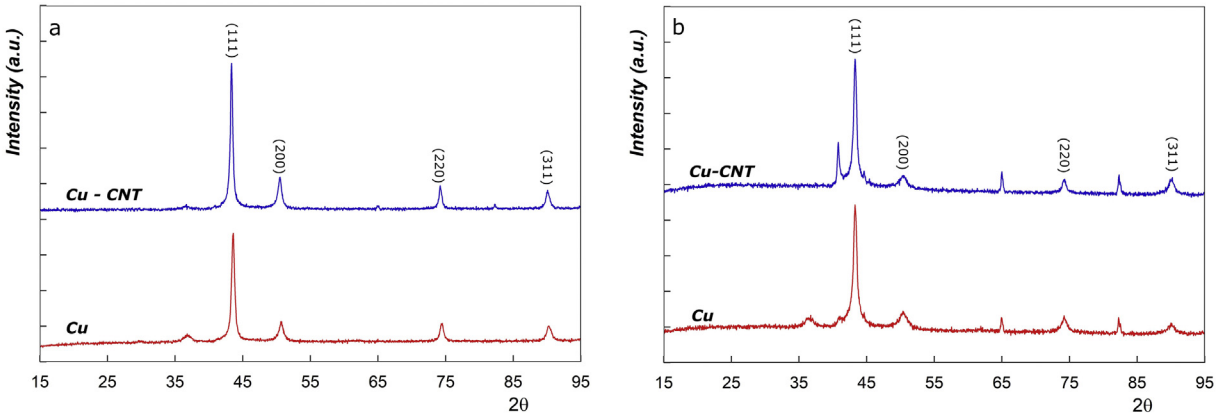

Fig. 7. XRD patterns of Cu (red line) and Cu-CNT (blue line) samples deposited (a) without BD and (b) after addition of 10 g/L of BD to the electrolyte. (For interpretation of the references to color in this figure legend, the reader is referred to the web version of this article.)

determine how they alter the composition of the electrolyte near the cathode surface. Moreover, the impact of these changes on the nucleation and growth processes will also depend on the bath formulation to which they are added. Hence, in the case of the Cu-CNT system, the change in texture could be explained by the growing mechanism proposed by Arai et al. [24,25]. Since CNT possess a high electrical conductivity, they act as additional nucleation sites meaning that Cu deposition takes place both on the steel substrate and CNTs. It is well known that the preferred crystal orientation of electrodeposited coatings is influenced by the substrate texture [50,51], therefore it could be expected that the presence of nanotubes in the growing metal led to a change in the preferential growth direction. Besides, current density distribution along the reaction surface will be affected by the embedded nanotubes generating high density peaks, which might also contribute to the change in microstructure [52]. Comparison of Fig. 8-a and -b reveals that BD considerably hindered growth along the [311] and [220] direction, favoring the development of a (111) texture as the one observed for Cu deposits obtained in the absence of US [37]. This result is not surprising considering that organic additives usually adsorb preferentially on specific crystal planes [53], changing their surface energy and hence the habit of crystals. Finally, Fig. 8-b also shows that even in the presence of BD, CNTs promoted the growth of copper deposits following the [311] direction.

XRD patterns were also used to estimate the average crystallite size (Table 1) following the procedure described previously. An appreciable decrease in this parameter was observed after addition of BD to the electrolyte, in accordance with results reported by Sekar [54] for deposition of Cu coatings from a sulfate bath in the presence of various additives. This behavior is typical for organic compounds known as grain refiners, which adsorb at the surface of the electrode, blocking active sites and hindering crystal growth; thus promoting the formation

Table 1
Crystallite size, tribological and mechanical properties of Cu and Cu-CNT deposits.

Coating	BD (g/L)	Crystallite size (Å)	Microhardness HV	COF	WD (10^{-4} mm^3/Nm)
Cu	–	150	189.1	0.148	7.69
Cu-CNT	–	180	200.7	0.127	2.16
Cu	10	100	284.7	0.179	5.43
Cu-CNT	10	120	243.8	0.153	3.24

of additional nucleus [53]. Regarding the effect on CNT, it was observed that incorporation of these particles to the copper matrix led to an increase in crystallite size. This is rather unexpected considering the trends reported previously for Cu-CNT deposits [27] which suggest that particles may act as additional active sites for the nucleation process, reducing the crystallite size of the deposit. Although this postulate is probably true for conducting particles such as CNT, it could also explain the rise in crystallite size found in this study. Taking into account the mechanism proposed by Arai et al. [24,25], the protruding tips of partially embedded CNT would not only become an available nucleation site but also an easily accessible spot for Cu^{2+} ions diffusing towards the electrode surface. Therefore, as a result of current distribution, deposition would likely occur at a higher rate at these tips than elsewhere in the reaction surface. This will only usually lead to an increase in the roughness of the coating [55], but under certain conditions dendritic growth could take place at these sites [56]. In that case, deposition at the tip of CNT would be under activation control generating larger highly regular copper crystallites [57,58] inside the coating. This electrochemical effect usually found during metal

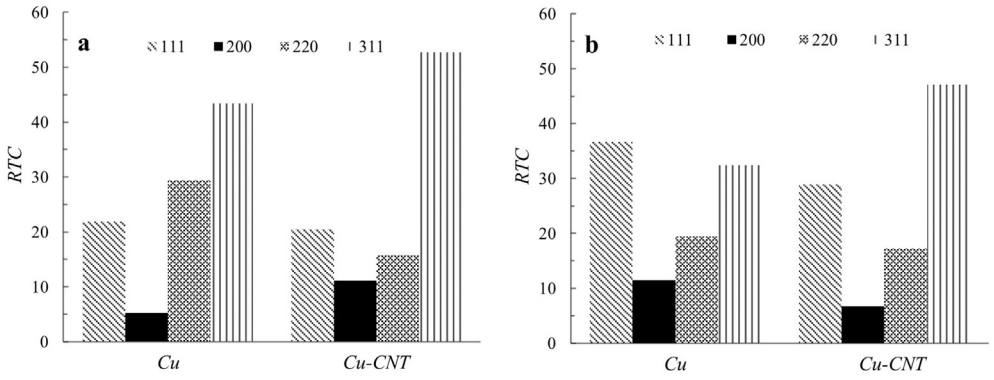

Fig. 8. RTC values of Cu and Cu-CNT deposits obtained (a) in absence and (b) in the presence of BD.

electrodeposition, would support an increase in the crystallite average size.

Table 1 also summarizes the mechanical and tribological properties of Cu and Cu-CNT coatings. As described in previous paragraphs both CNT and BD have an impact on the **COF** value of these samples. Likewise, changes in the deposit's microhardness were registered after particle incorporation and addition of the additive to the electrolyte. It can be seen that BD led to a 50% increase in the microhardness of pure copper deposits, probably as a result of a grain refinement effect. The results also show that the influence of CNT on this parameter depended on whether BD was present or not in the solution. In this regard, a slight increase was observed after particle incorporation in the absence of BD, while in the presence of this compound CNTs led to a reduction of microhardness. These trends suggest that incorporation of CNT has two opposing effects in the microstructure and mechanical properties of Cu. On the one hand, a dispersed phase can lead to an increase in coating microhardness by a dispersion strengthening mechanism [9,59]. On the other hand, incorporation of CNT caused a rise in crystallite size of Cu deposits which might bring about a decrease in coatings microhardness. Based on the reported results, it can be concluded that in the absence of BD the first effect is the dominant one, while the refinement of microstructure governs the changes in microhardness of deposits obtained from an electrolyte containing BD.

The WDs calculated according to the ASTM G99 show that CNT incorporation significantly improved the Cu wear resistance, in agreement with results obtained for composites prepared by powder metallurgy [4,23]. Although the higher microhardness of Cu-CNT may contribute to the improvement in tribological performance, the large differences in WD cannot be only ascribed to this. It is likely that loose nanotubes between the contact surfaces, which would prevent their intimate contact, also contribute to the decrease in wear rate as suggested by Tu et al. [5]. Similar changes were observed for deposits obtained in the presence of BD, although the improvement in wear resistance was less significant in this case, probably due to the decrease in microhardness caused by incorporation of CNTs.

SEM images of the wear tracks (Fig. 9-a) revealed the presence of several grooves aligned with the sliding direction characteristic of ploughing. The latter is indicative of an abrasive wear mechanism [60] of a soft material by a hard surface [61], consistent with the difference in hardness between the coating material and the counter body. Moreover, some cracks (red arrows) and loose flakes (blue circles) were detected in the worn surface, which suggest that the samples could have undergone some delamination during the test [62,63]. The same wear mechanism was observed for Cu and Cu-CNT obtained either in the presence or the absence of BD, although some differences should be remarked. First, Cu coatings deposited from an electrolyte without BD presented larger grooves (Fig. 9-b), confirming the higher wear rate estimated previously for this sample. The latter is not surprising considering this deposit showed the lowest microhardness. In contrast, after addition of BD only some thin scratches are visible on the wear track (Fig. 9-c), although a considerable number of cracks can be observed, which may arise from the higher microhardness, and thus higher brittleness, of this sample. No significant differences were detected between composites obtained with or without addition of BD, suggesting that for these materials the wear mechanism is primarily determined by the presence of CNT between the mating surfaces rather than the metal properties. Finally, no evidence of adhesive wear was found consistent with the absence of a transfer on the counterbody.

To further characterize the morphology of the worn surface, 3D images and profiles of the four samples were recorded with an optical profilometer. These measurements showed that the wear tracks of copper coatings (Fig. 10-a and -c) have a well-defined spherical shape indicative of a conformal wear. Moreover, profile analysis yielded a cross-section area of the wear track almost identical to that calculated following the procedure detailed in the ASTM G99 standard. In contrast, relatively flat (not rounded) wear tracks, were observed for Cu-CNT composites (Fig. 10-b and -d), suggesting that penetration of the counter body occurs only to a small extent. Comparison of the cross-sectional area values calculated from the profile and the formula in the standard, showed that the latter overestimates the wear degree by a 4.8 and 2.7 factor for composites obtained in the absence and the presence of BD, respectively. Therefore, these results suggest that calculation of the WD with the ASTM G99 procedure may be used for comparative purposes only, but a detailed profile characterization is necessary to obtain a precise estimation of the wear rate.

4. Conclusions

In the present study, Cu-CNT composites coatings with good tribological and mechanical properties were obtained by US-assisted electrodeposition from a recently developed alkaline cyanide-free electrolyte. The results showed that particle incorporation can be achieved at several temperatures and current densities both in the absence and the presence of BD. Regardless of experimental conditions, composite coatings always presented a lower **COF** than pure Cu confirming the lubricating properties of CNT. However, deposition parameters strongly influenced the tribological behavior of pure Cu and composite coatings and therefore these should be chosen carefully in order to attain the best performance.

Detailed microstructure analysis revealed that incorporation of CNT induces changes in the surface morphology as well as in the preferred crystal orientation, promoting crystal growth along the [311] direction.

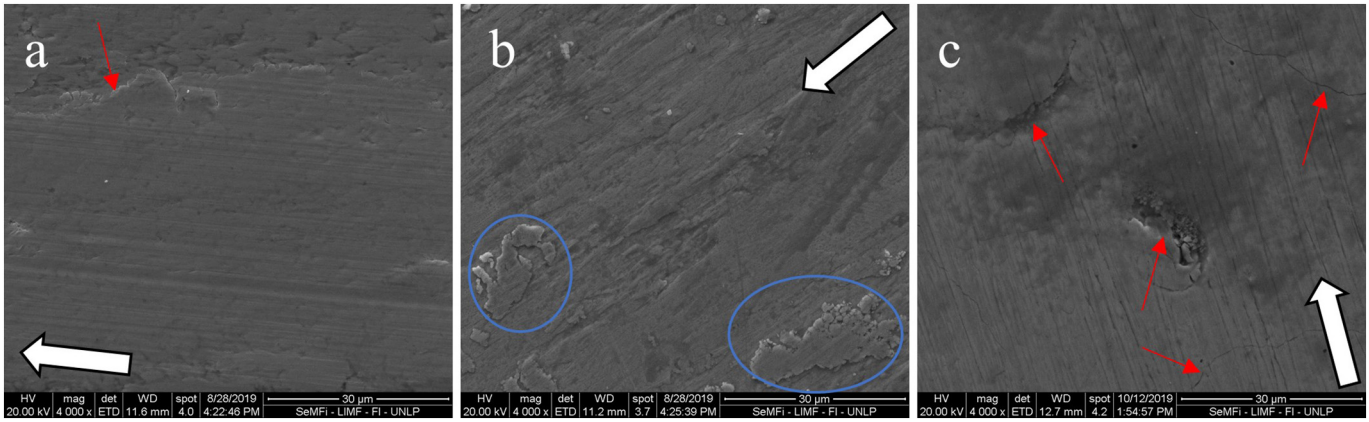

Fig. 9. SEM images (4000×) of the wear track of (a) Cu-CNT and (b) Cu obtained from a bath without BD; (c) Cu deposits obtained after addition of 10 g/L of BD. White arrows indicate the sliding direction during the test. (For interpretation of the references to color in this figure, the reader is referred to the web version of this article.)

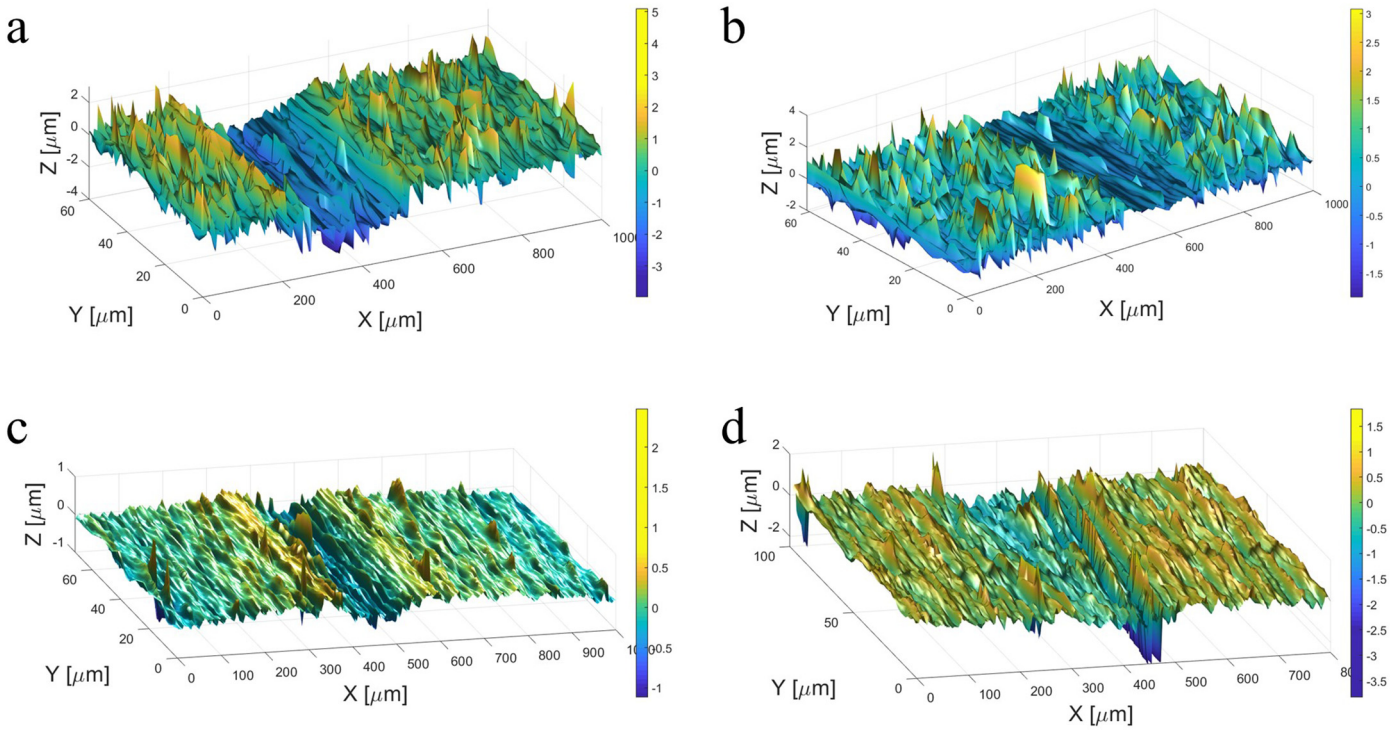

Fig. 10. 3D images of the wear track of Cu and Cu-CNT coatings deposited at 3 A/dm^2 and 45 °C on smooth substrates in the absence of BD: (a) Cu and (b) Cu-CNT; and in the presence of BD: (c) Cu and (d) Cu-CNT.

Likewise, BD affected both the morphology (minimizing cracks formation) and the texture of the deposits as a result of additive specific adsorption. XRD studies also showed that BD had a grain refinement effect, which accounts for the increase in microhardness caused by this additive. In contrast, CNT led to an increase in crystallite size possibly by a growth mechanism taking place on the tip of these particles similar to dendritic growth.

The differences in microstructure and microhardness of pure Cu coatings obtained with and without BD, led to rather different wear rates. Nevertheless, this additive had little influence on the wear resistance of Cu-CNT composites. It was proposed that for this material the wear mechanism is predominantly determined by the presence of CNT between the mating surfaces rather than its physical properties. The latter significantly reduces the wear rate in comparison to pure Cu coatings. For this reason, it can be concluded that incorporation of CNT considerably improves the mechanical properties and wear resistance of copper, backing the use of the approach considered in this study to prepared self-lubricating coatings.

Despite leading to a significant decrease in WD, addition of BD to the electrolyte had a detrimental effect on the **COF** value. Therefore, this additive should not be included in the bath formulation to reach the best tribological performance. However, the use of organic additives to further enhance the wear resistance of Cu-CNT must not be discarded, and will be considered in future investigations.

CRediT authorship contribution statement

Leandro N. Bengoa: Conceptualization, Investigation, Formal Analysis, Writing - original draft. **Pablo R. Seré:** Conceptualization, Investigation, Formal Analysis, Writing - review & editing. **Paola Pary:** Investigation, Writing - review & editing. **M. Susana Conconi:** Investigation. **José M. Folgueiras:** Investigation, Software. **Eneas N. Morel:** Methodology. **Jorge Torga:** Investigation, Software. **Walter A. Egli:** Supervision, Resources, Writing - review & editing.

Declaration of competing interest

The authors declare that they have no known competing financial interests or personal relationships that could have appeared to influence the work reported in this paper.

Acknowledgment

The authors would like to thank Comisión de Investigaciones Científicas de la Provincia de Buenos Aires (CICPBA), Consejo Nacional de Investigaciones Científicas y Técnicas (CONICET), Agencia Nacional de Promoción Científica y Tecnológica (PICT 2015-3819) and Universidad Nacional de La Plata (UNLP) for the funds and support provided for this investigation. Cheaptubes is also acknowledged for providing the carbon nanotubes used in this study.

References

[1] M. Ghorbani, M. Mazaheri, A. Afshar, Wear and friction characteristics of electrodeposited graphite–bronze composite coatings, Surf. Coatings Technol. 190 (2005) 32–38.
[2] H.E. Sliney, The use of silver in self-lubricating coatings for extreme temperatures, A S L E Trans 29 (1986) 370–376, https://doi.org/10.1080/05698198608981698.
[3] L. Rapoport, M. Lvovsky, I. Lapsker, V. Leshchinsky, Y. Volovik, Y. Feldman, A. Margolin, R. Rosentsveig, R. Tenne, Slow release of fullerene-like WS2 nanoparticles from Fe – Ni graphite matrix: a self-lubricating nanocomposite, Nano Lett. 1 (2001) 137–140, https://doi.org/10.1021/nl005516v.
[4] W.X. Chen, J.P. Tu, L.Y. Wang, H.Y. Gan, Z.D. Xu, X.B. Zhang, Tribological application of carbon nanotubes in a metal-based composite coating and composites, Carbon N. Y. 41 (2003) 215–222, https://doi.org/10.1016/S0008-6223(02)00265-8.
[5] L.Y. Wang, J.P. Tu, W.X. Chen, Y.C. Wang, X.K. Liu, C. Olk, D.H. Cheng, X.B. Zhang, Friction and wear behavior of electroless Ni-based CNT composite coatings, Wear 254 (2003) 1289–1293, https://doi.org/10.1016/S0043-1648(03)00171-6.
[6] A. Afshar, M. Ghorbani, M. Mazaheri, Electrodeposition of graphite-bronze composite coatings and study of electroplating characteristics, Surf. Coatings Technol. 187 (2004) 293–299.
[7] T. Nickchi, M. Ghorbani, Pulsed electrodeposition and characterization of bronze-graphite composite coatings, Surf. Coatings Technol. 203 (2009) 3037–3043.
[8] T. Nickchi, M. Ghorbani, A. Alfantazi, Z. Farhat, Fabrication of low friction bronze–graphite nano-composite coatings, Mater. Des. 32 (2011) 3548–3553.

[9] J.P. Celis, J.R. Roos, C. Buelens, J. Fransaer, Mechanism of electrolytic composite plating: survey and trends, Trans. Inst. Met. Finish. 69 (1991).
[10] J.L. Stojak, J. Fransaer, J.B. Talbot, Review of electrocodeposition, in: R.C. Alkire, D.M. Kolb (Eds.), Adv. Electrochem. Sci. Eng. Wiley-VCH, Germany, 2002.
[11] A. Hovestad, L.J.J. Janssen, Electrochemical codeposition of inert particles in a metallic matrix, J. Electrochem. Soc. 25 (1995) 519–527.
[12] C.G. Fink, J.D. Prince, The codeposition of copper and graphite, Trans. Am. Electrochem. Soc. 54 (1928) 315.
[13] E. Pena-Munoz, P. Berçot, A. Grosjean, M. Rezrazi, J. Pagetti, Electrolytic and electroless coatings of Ni–PTFE composites: study of some characteristics, Surf. Coatings Technol. 107 (1998) 85–93, https://doi.org/10.1016/S0257-8972(98)00547-7.
[14] P. Berçot, E. Peña-Muñoz, J. Pagetti, Electrolytic composite Ni–PTFE coatings: an adaptation of Guglielmi's model for the phenomena of incorporation, Surf. Coatings Technol. 157 (2002) 282–289.
[15] L. Shi, C. Sun, W. Liu, Electrodeposited nickel–cobalt composite coating containing MoS2, Appl. Surf. Sci. 254 (2008) 6880–6885, https://doi.org/10.1016/j.apsusc.2008.04.089.
[16] M.F. Cardinal, P.A. Castro, J. Baxi, H. Liang, F.J. Williams, Characterization and frictional behavior of nanostructured Ni–W–MoS2 composite coatings, Surf. Coatings Technol. 204 (2009) 85–90, https://doi.org/10.1016/j.surfcoat.2009.06.037.
[17] M.M.J. Treacy, T.W. Ebbesen, J.M. Gibson, Exceptionally high Young's modulus observed for individual carbon nanotubes, Nature 381 (1996) 678–680, https://doi.org/10.1038/381678a0.
[18] P.L. Dickrell, S.B. Sinnott, D.W. Hahn, N.R. Raravikar, L.S. Schadler, P.M. Ajayan, W.G. Sawyer, Frictional anisotropy of oriented carbon nanotube surfaces, Tribol. Lett. 18 (2005) 59–62, https://doi.org/10.1007/s11249-004-1752-0.
[19] S. Arai, A. Fujimori, M. Murai, M. Endo, Excellent solid lubrication of electrodeposited nickel-multiwalled carbon nanotube composite films, Mater. Lett. 62 (2008) 3545–3548, https://doi.org/10.1016/j.matlet.2008.03.047.
[20] X.. Chen, F.. Cheng, S.. Li, L.. Zhou, D.. Li, Electrodeposited nickel composites containing carbon nanotubes, Surf. Coatings Technol. 155 (2002) 274–278, https://doi.org/10.1016/S0257-8972(02)00118-4.
[21] C.R. Carpenter, P.H. Shipway, Y. Zhu, D.P. Weston, Effective dispersal of CNTs in the fabrication of electrodeposited nanocomposites, Surf. Coatings Technol. 205 (2011) 4832–4837, https://doi.org/10.1016/j.surfcoat.2011.04.070.
[22] Y. Suzuki, S. Arai, M. Endo, Electrodeposition of Ni–P alloy–multiwalled carbon nanotube composite films, J. Electrochem. Soc. 157 (2010) D50, https://doi.org/10.1149/1.3254180.
[23] J.P.P. Tu, Y.Z.Z. Yang, L.Y.Y. Wang, X.C.C. Ma, X.B.B. Zhang, Tribological properties of carbon-nanotube-reinforced copper composites, Tribol. Lett. 10 (2001) 225–228, https://doi.org/10.1023/A:1016662114589.
[24] S. Arai, T. Saito, M. Endo, Cu–MWCNT composite films fabricated by electrodeposition, J. Electrochem. Soc. 157 (2010) D147, https://doi.org/10.1149/1.3280034.
[25] S. Arai, T. Saito, M. Endo, Effects of additives on Cu-MWCNT composite plating films, J. Electrochem. Soc. 157 (2010) D127, https://doi.org/10.1149/1.3274202.
[26] S. Fu, X. Chen, P. Liu, W. Liu, P. Liu, K. Zhang, H. Chen, Electrodeposition and properties of composites consisting of carbon nanotubes and copper, J. Mater. Eng. Perform. 27 (2018) 5511–5517, https://doi.org/10.1007/s11665-018-3623-0.
[27] Y.L. Yang, Y.D. Wang, Y. Ren, C.S. He, J.N. Deng, J. Nan, J.G. Chen, L. Zuo, Single-walled carbon nanotube-reinforced copper composite coatings prepared by electrodeposition under ultrasonic field, Mater. Lett. 62 (2008) 47–50, https://doi.org/10.1016/J.MATLET.2007.04.086.
[28] Z. An, M. Toda, T. Ono, Comparative investigation into surface charged multi-walled carbon nanotubes reinforced Cu nanocomposites for interconnect applications, Compos. Part B Eng. 95 (2016) 137–143, https://doi.org/10.1016/J.COMPOSITESB.2016.03.086.
[29] Y. Feng, G.E. McGuire, O.A. Shenderova, H. Ke, S.L. Burkett, Fabrication of copper/carbon nanotube composite thin films by periodic pulse reverse electroplating using nanodiamond as a dispersing agent, Thin Solid Films 615 (2016) 116–121, https://doi.org/10.1016/J.TSF.2016.07.015.
[30] A. Singh, T. Ram Prabhu, A.R. Sanjay, V. Koti, An overview of processing and properties of CU/CNT nano composites, Mater. Today Proc. 4 (2017) 3872–3881, https://doi.org/10.1016/J.MATPR.2017.02.286.
[31] R.M. Sundaram, A. Sekiguchi, M. Sekiya, T. Yamada, K. Hata, Copper/carbon nanotube composites: research trends and outlook, R. Soc. Open Sci. 5 (2018) 180814, , https://doi.org/10.1098/rsos.180814.
[32] E. García-Lecina, I. García-Urrutia, J.A. Díez, J. Morgiel, P. Indyka, A comparative study of the effect of mechanical and ultrasound agitation on the properties of electrodeposited Ni/Al2O3 nanocomposite coatings, Surf. Coatings Technol. 206 (2012) 2998–3005, https://doi.org/10.1016/j.surfcoat.2011.12.037.
[33] I. Tudela, Y. Zhang, M. Pal, I. Kerr, A.J. Cobley, Ultrasound-assisted electrodeposition of composite coatings with particles, Surf. Coatings Technol. 259 (2014) 363–373, https://doi.org/10.1016/j.surfcoat.2014.06.023.
[34] I. Tudela, Y. Zhang, M. Pal, I. Kerr, A.J. Cobley, Ultrasound-assisted electrodeposition of thin nickel-based composite coatings with lubricant particles, Surf. Coatings Technol. 276 (2015) 89–105, https://doi.org/10.1016/j.surfcoat.2015.06.030.
[35] M.K. Camargo, I. Tudela, U. Schmidt, A.J. Cobley, A. Bund, Ultrasound assisted electrodeposition of Zn and Zn-TiO2 coatings, Electrochim. Acta 198 (2016) 287–295, https://doi.org/10.1016/j.electacta.2016.03.078.
[36] L.N. Bengoa, A. Ispas, J.F. Bengoa, A. Bund, W.A. Egli, Ultrasound assisted electrodeposition of Cu-SiO_2 composite coatings: effect of particle surface chemistry, J. Electrochem. Soc. 166 (2019) D244–D251, https://doi.org/10.1149/2.0181908jes.
[37] P. Pary, L.N. Bengoa, W.A. Egli, Electrochemical characterization of a Cu(II)-glutamate alkaline solution for copper electrodeposition, J. Electrochem. Soc. 162 (2015) D275–D282, https://doi.org/10.1149/2.0811507jes.
[38] I. Tudela, Y. Zhang, M. Pal, I. Kerr, T.J. Mason, A.J. Cobley, Ultrasound-assisted electrodeposition of nickel: effect of ultrasonic power on the characteristics of thin coatings, Surf. Coatings Technol. 264 (2015) 49–59, https://doi.org/10.1016/j.surfcoat.2015.01.020.
[39] L.P. Bérubé, G. L'Espérance, A quantitative method of determining the degree of texture of zinc electrodeposits, J. Electrochem. Soc. 136 (1989) 2314–2315 http://jes.ecsdl.org/content/136/8/2314.abstract.
[40] M.L. Dufour, G. Lamouche, V. Detalle, B. Gauthier, P. Sammut, Low-coherence interferometry - an advanced technique for optical metrology in industry, Insight Non-Destructive Test. Cond. Monit. 47 (2005) 216–219, https://doi.org/10.1784/insi.47.4.216.63149.
[41] E. Morel, J.R. Torga, P.M. Tabla, M. Sallese, Reduction of measurement errors in OCT scanning, SPIE-Intl Soc Optical Eng, 2018, p. 13, , https://doi.org/10.1117/12.2282108.
[42] L.N. Bengoa, W.R. Tuckart, N. Zabala, G. Prieto, W.A. Egli, Bronze electrodeposition from an acidic non-cyanide high efficiency electrolyte: tribological behavior, Surf. Coatings Technol. 253 (2014) 241–248, https://doi.org/10.1016/j.surfcoat.2014.05.046.
[43] J. Fransaer, J.P. Celis, J.R. Roos, Analysis of the electrolytic codeposition of non-brownian particles with metals, J. Electrochem. Soc. 139 (1992) 413–425.
[44] B.E. Conway, Theory and Principles of Electrode Processes, Ronald Press Co, New York, 1965.
[45] J.O. Bockris, A.K.N. Reddy, Modern Electrochemistry, Plenum Press, New York, 1970, pp. 623–844.
[46] B.B. Damaskin, O.A. Petrii, V.V. Batrakov, Adsorption of Organic Compounds on Electrodes, (1971) (New York - London).
[47] M.K. Camargo, U. Schmidt, R. Grieseler, M. Wilke, A. Bund, Electrodeposition of Zn-TiO2 dispersion coatings: study of particle incorporation in chloride and sulfate baths, J. Electrochem. Soc. 161 (2014) D168–D175, https://doi.org/10.1149/2.066404jes.
[48] Y. Raghupathy, A. Kamboj, M.Y. Rekha, N.P. Narasimha Rao, C. Srivastava, Copper-graphene oxide composite coatings for corrosion protection of mild steel in 3.5% NaCl, Thin Solid Films 636 (2017) 107–115, https://doi.org/10.1016/j.tsf.2017.05.042.
[49] E.A. Pavlatou, N. Spyrellis, Influence of pulse plating conditions on the structure and properties of pure and composite nickel nanocrystalline coatings, Russ. J. Electrochem. 44 (2008) 745–754, https://doi.org/10.1134/S1023193508060165.
[50] R. Winand, Electrodeposition of metals and alloys-new results and perspectives, Electrochim. Acta 39 (1994) 1091–1105, https://doi.org/10.1016/0013-4686(94)E0023-S.
[51] H.J. Pick, G.G. Storey, T.B. Vaughan, The structure of electrodeposited copper-I. An experimental study of the growth of copper during electrodeposition, Electrochim. Acta 2 (1960) 165–176, https://doi.org/10.1016/0013-4686(60)87014-4.
[52] X. Ye, M. De Bonte, J.P. Celis, J.R. Roos, Role of overpotential on texture, morphology and ductility of electrodeposited copper foils for printed circuit board applications, J. Electrochem. Soc. 139 (1992) 1592–1600, https://doi.org/10.1149/1.2069461.
[53] L. Oniciu, L. Mureşan, Some fundamental aspects of levelling and brightening in metal electrodeposition, J. Appl. Electrochem. 21 (1991) 565–574, https://doi.org/10.1007/BF01024843.
[54] R. Sekar, Synergistic effect of additives on electrodeposition of copper from cyanide-free electrolytes and its structural and morphological characteristics, Trans. Nonferrous Met. Soc. China (English Ed.) 27 (2017) 1665–1676, https://doi.org/10.1016/S1003-6326(17)60189-4.
[55] K.I. Popov, M.G. Pavlovic, M.D. Maksimovic, Comparison of the critical conditions for initiation of dendritic growth and powder formation in potentiostatic and galvanostatic copper electrodeposition, J. Appl. Electrochem. 12 (1982) 525–531.
[56] K.I. Popov, N.D. Nikolic, General theory of disperse metal electrodeposits formation, in: S.S. Djokić (Ed.), Electrochem. Prod. Met. Powders, Springer Science +Business Media, New York, 2012, pp. 1–62.
[57] N.D. Nikolić, G. Branković, U.Č. Lačnjevac, Formation of two-dimensional (2D) lead dendrites by application of different regimes of electrolysis, J. Solid State Electrochem. 16 (2012) 2121–2126, https://doi.org/10.1007/s10008-011-1626-y.
[58] N.D. Nikolić, K.I. Popov, P.M. Živković, G. Branković, A new insight into the mechanism of lead electrodeposition: ohmic-diffusion control of the electrodeposition process, J. Electroanal. Chem. 691 (2013) 66–76, https://doi.org/10.1016/j.jelechem.2012.12.011.
[59] M.J.L. Gines, F.J. Williams, C.A. Schuh, Nanostructured Cr-C coatings for application at high temperatures, J. Appl. Surf. Finish. 2 (2007) 112–121.
[60] W.M. Garrison, Abrasive wear resistance: the effects of ploughing and the removal of ploughed material, Wear 114 (1987) 239–247, https://doi.org/10.1016/0043-1648(87)90090-1.
[61] D. Arnell, Mechanisms and laws of friction and wear, Tribol. Dyn. Engine Powertrain Fundam. Appl. Futur. Trends, Elsevier Ltd, 2010, pp. 41–72, , https://doi.org/10.1533/9781845699932.1.41.
[62] N.P. Suh, An overview of the delamination theory of wear, Wear 44 (1977) 1–16, https://doi.org/10.1016/0043-1648(77)90081-3.
[63] R. Karslioglu, H. Akbulut, Comparison microstructure and sliding wear properties of nickel–cobalt/CNT composite coatings by DC, PC and PRC current electrodeposition, Appl. Surf. Sci. 353 (2015) 615–627, https://doi.org/10.1016/j.apsusc.2015.06.161.